THE JOURNAL OF PHYSICAL CHEMISTRY B

Article

pubs.acs.org/JPCB

Effects of Surfactants on the Purple Membrane and Bacteriorhodopsin: Solubilization or Aggregation?

Ka Chon Ng and Li-Kang Chu*

Department of Chemistry, National Tsing Hua University, 101, Sec. 2, Kuang-Fu Rd., Hsinchu 30013, Taiwan

Supporting Information

ABSTRACT: Using steady-state spectroscopic and zeta potential methods, we have unraveled the interaction of the purple membrane (PM) and bacteriorhodopsin (bR) with various surfactants below their critical micelle concentrations. We found that the charged hydrophilic heads of ionic surfactants play a role in perturbing the structure and conformation of PM and bR and that ionic surfactants of opposite charges cause opposing effects. Specifically, the addition of a low concentration (0.2 mM) of the cationic surfactant cetyl trimethylammonium bromide (CTAB) is capable of neutralizing the negatively charged lipids on the PM surface via electrostatic forces. This results in increased hydrophobicity of PM that leads to the aggregation of PM. In contrast, denaturation of PM and bR was observed when the anionic surfactant sodium dodecyl sulfate (SDS) was added to the PM suspensions. The attachment of SDS to the PM surface increases the solubility of PM and causes a loose crystalline structure. As the SDS concentration is increased to more than 3 mM, the secondary structure of the constituents of bR is significantly distorted, and the protonated Schiff base is hydrolyzed to form free retinal. The addition of the neutral surfactant diethylene glycol mono-*n*-hexyl ether (C6E2) does not significantly influence the PM and bR, meaning most of their original properties are preserved. We conclude that the addition of surfactants might cause the aggregation or solubilization of the membrane protein, depending on the signs of the charged hydrophilic heads of the surfactants and the charges of the membrane protein surface. Aggregation results when the surfactant and protein have opposite charges, whereas solubilization results when the surfactant and protein have the same charge.

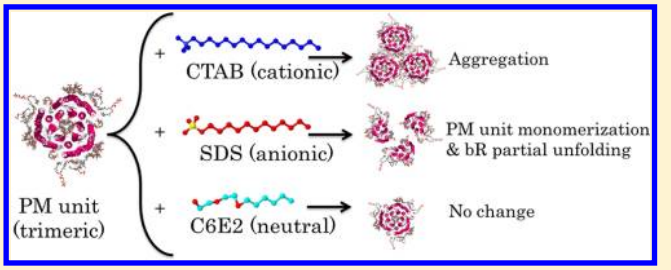

1. INTRODUCTION

Bacteriorhodopsin (bR), a constituent protein on the membrane of the halophile *Halobacterium salinarum*, has been regarded as a prototypical photosynthetic system.[1,2] bR is composed of seven α-helices and one retinal, which covalently binds to Lys-216 to form the protonated Schiff base. The photoexcitation of the retinal moiety initiates a photocycle that generates a proton gradient between the cytoplasmic and extracellular sides of bR.[2] Three bR units and ten lipids per bR form a stable trimeric structure in the 2D hexagonal lattice that is the primitive unit of the purple membrane (PM).[3] The native lipids in PM are mostly polar, except for the nonpolar lipid squalene, and are in the forms of phosphatidyl glycerol phosphate (PGP) and glycolipid sulfate (GLS), both of which have hydrophobic tails formed from archaeol, a branched saturated hydrocarbon chain.[4] The lipids in PM can be categorized into four classes in terms of their locations: (1) the PGP lipids located at the extratrimer, (2) the squalene at the extratrimer, (3) the GLS on the extracellular side at the intratrimer, and (4) the PGP on the cytoplasmic side at the intratrimer, where the extratrimer and intratrimer denote the periphery of the trimeric bR and the cavity within this trimer, respectively.[5] The individual lipids play specific roles in the photocycle of bR and the subsequent proton pumping.[6−8]

It has been found that the addition of various surfactants alters the configuration of the PM, resulting in effects such as delipidation and monomerization, and extensive studies have been carried out to investigate the difference in the photocycle of the monomeric bR and delipidated PM.[10−12] del Río et al. have demonstrated that the solubilization and bleaching of bR was highly associated with the steric hindrance of the hydrophobic tails and the charged heads of the surfactants.[9] Previous reports have shown that neutral surfactants are relatively mild and only lead to the delipidation or monomerization of PM without significant denaturing of bR.[10−13] The addition of the nonionic surfactant Triton X-100 solubilizes the native trimeric bR and leads to the generation of the monomeric bR, which was characterized as a peak ca. 553 nm in the visible spectrum.[10,11] Furthermore, the kinetics of the retinal isomerization of the light-adapted form of bR were decelerated,[11] but the deprotonation of the protonated Schiff base was significantly accelerated.[12] Upon addition of the zwitterionic surfactant 3-[(3-cholamidopropyl)-dimethylammonio]-1-propanesulfonate (CHAPS), the native lipids of PM were partially removed, leaving only 25% (by

Received: February 4, 2013
Revised: April 9, 2013
Published: April 9, 2013

   dx.doi.org/10.1021/jp401254j | J. Phys. Chem. B 2013, 117, 6241−6249

weight) of the lipids intact, and the bR in the delipidated PM exhibits an absorption maximum at 560 nm.[13] The corresponding proton pump decay kinetics was greatly decelerated.[12] Besides neutral surfactants, the photocycle of bR in PM has been proven to be perturbed in the presence of ionic surfactants in different fashions, depending on the signs of the charges of the hydrophilic heads and the length of the hydrophobic tails.[14,15]

Dose-dependent studies have been carried out to unravel the roles of surfactants in changing the configuration of bR and PM.[16,17] Tan and Birge have studied the interaction of bR with micelles of cationic alkylammonium surfactants and found that the solubilization rate of PM was dependent on the micellular environment, specifically the length of the surfactant tail and the size and hydrophobicity of the headgroup.[16] Padrós et al. have indicated that the addition of the anionic surfactant sodium dodecyl sulfate below its critical micelle concentration (CMC) leads to the generation of a blue form of bR (λ_{max} = 600 nm).[17] However, pulsed electron paramagnetic resonance spectroscopy revealed that the bR in the SDS micelle rarely retained its native tertiary structure and instead existed in a heterogeneous ensemble of different secondary structures.[18] Although the alteration of the retinal moiety has been studied by using steady-state absorption spectroscopy in the visible region, the alteration of the secondary structure of bR at the molecular level has not been sufficiently investigated.[16,17]

In this work, we have employed steady-state UV−vis absorption, fluorescence, circular dichroism (CD), and infrared absorption spectroscopies to determine the alteration of the configurations of PM and bR upon the addition of various surfactants. We observed that the cationic surfactant CTAB interacts with the lipids in PM via the electrostatic forces between the oppositely charged heads of CTAB and the lipids. The subsequent neutralization of the surface charge of the PM reduced its solubility and thus leads to significant PM aggregation. Alternatively, the anionic surfactant SDS attaches to the PM surface via the hydrophobic interaction between the hydrocarbon tails of the lipids and SDS, and the accumulation of the negatively charged sulfate head of SDS thereby increases the solubility of PM, which leads to the monomerization of the trimeric configuration. The monomeric bR then undergoes further denaturing upon the addition of more SDS. The addition of the neutral surfactant C6E2 did not perturb the structures of PM and bR in a significant fashion.

2. MATERIALS AND METHODS

2.1. Sample Preparation. The PM fragments of the S9 strain of *H. salinarium* were prepared according to a known method.[19] Pure PM suspensions were irradiated with light for 1 h to ensure the formation of light-adapted bR before mixing with the surfactants. Three surfactants, cetyl trimethylammonium bromide (CTAB, Alfa Aesar, 98%), sodium dodecyl sulfate (SDS, Sigma-Aldrich, >98.5%), and diethylene glycol mono-*n*-hexyl ether (C6E2, TCI America, 95%), were each mixed with the PM suspensions. The corresponding structures of the surfactants are shown in Figure 1. The concentration of constituent bR was controlled at 20 μM, as determined spectroscopically by the extinction coefficient of 62 700 M^{-1} cm^{-1} at 568 nm.[20] The pH was controlled at 7.4 (phosphate buffer solution, Sigma-Aldrich, 1.0 M), and the buffer was diluted to 50 μM. The concentrations of the surfactants were controlled below their CMCs. The mixtures of PM and surfactants were prepared freshly and the spectroscopic

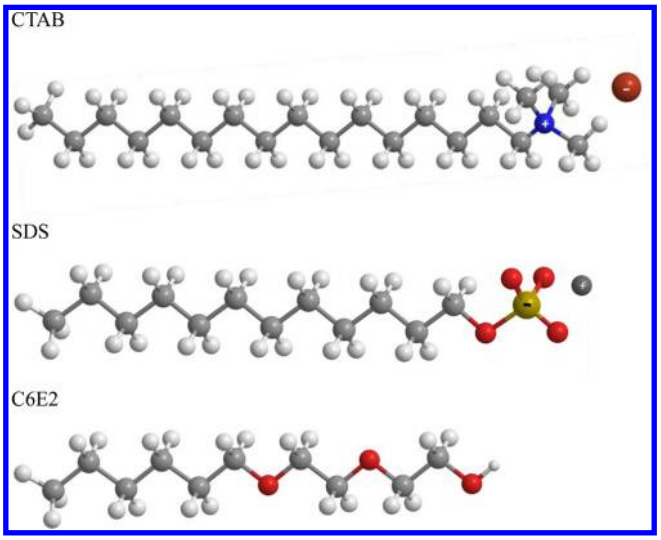

Figure 1. Structures of the surfactants CTAB, SDS, and C6E2.

measurements were carried out after the mixtures were allowed to react for 30 min under illumination. Parts of the surfactant-treated PM solutions were further centrifuged at 18 400*g* for 15 min to investigate the difference of the spectroscopic behaviors of the supernatants and pellets. Upon examination of the ultraviolet−visible absorption spectra and the fluorescence spectra, it was found that a small but ultimately insignificant amount of PM remained in the supernatants of the solutions treated with CTAB and C6E2. The supernatant of the SDS-treated PM exhibits a slight yellowish color indicating the generation of the free retinal, and thus it is further concentrated using a centrifugal filter (Pall Corp., MWCO = 10 000) at 6000*g* for 10 min to remove the buffer and the solubilized SDS. The pellets of the CTAB- and C6E2-treated PM and the supernatant concentrate of the SDS-treated PM were redispersed on a CaF_2 window and dried at 25 °C under vacuum for further infrared absorption measurements.

2.2. Steady-State Spectroscopic Measurements. Steady-state spectroscopies are utilized to characterize and differentiate the structural alteration of bR and PM before and after the addition of surfactants. Ultraviolet−visible (UV−vis) absorption spectra were monitored with a USB4000-UV−vis Ocean Optics spectrometer. A cuvette with an optical path length of 1 mm was employed in the measurements of the aqueous samples. CD spectra were recorded over 700−450 at 1 nm intervals and averaged for 5 s with a model 410 AVIV spectrometer at 25 °C. Fluorescence (FL) spectra were collected with an F-7000 Hitachi spectrophotometer using a quartz cuvette with an optical path of 1 mm at 25 °C. The emission was recorded from 290 to 450 nm with scanning steps of 1 nm upon excitation at 280 nm. The surfactant-treated PM pellets were dispersed on a CaF_2 window for the infrared absorption measurements with a Fourier-transform infrared spectrometer (Vertex 80, Bruker). The spectra were acquired from 900 to 3600 cm^{-1} with a spectral resolution of 0.5 cm^{-1}, and each spectrum was averaged for 400 scans.

2.3. Zeta Potential Measurements. The zeta potentials measurements of the pure PM and surfactant-treated PM were carried out using a zeta potential analyzer (ZetaPlus, Brookhaven Instruments). The samples, containing PM and surfactants, were freshly prepared. The temperature and the pH were controlled at 25 °C and 7.4. Fifteen cycles were averaged

dx.doi.org/10.1021/jp401254j | J. Phys. Chem. B 2013, 117, 6241−6249

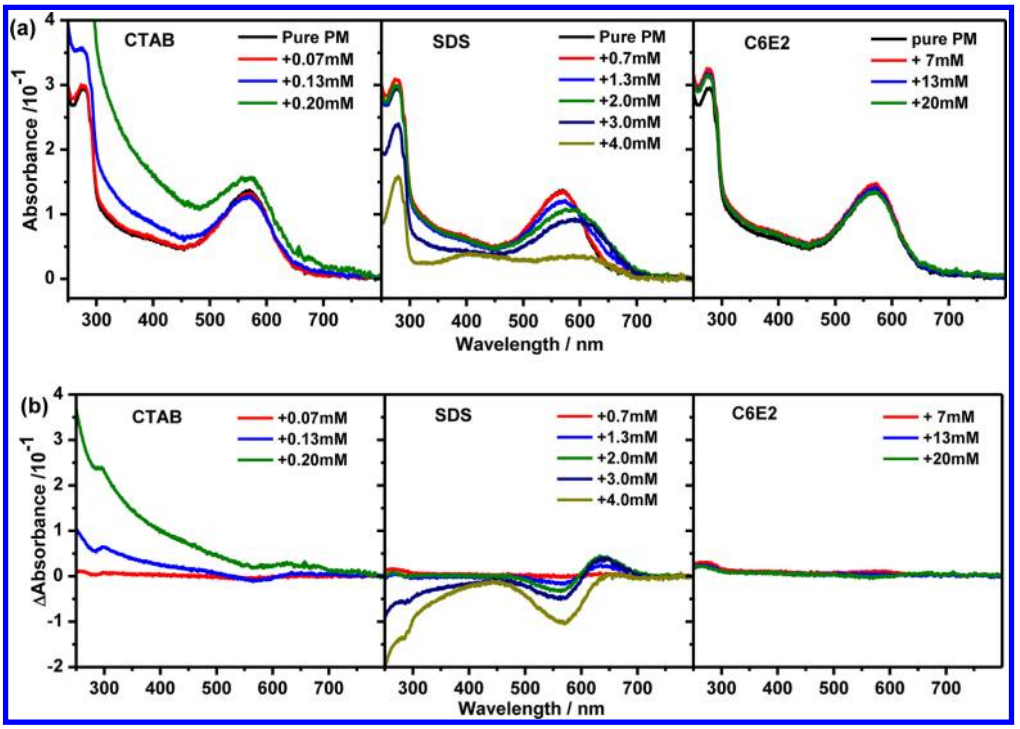

Figure 2. (a) Steady-state UV−vis absorption spectra of the mixtures containing PM and surfactants at varied concentrations after mixing for 30 min. (b) Difference spectra of the mixtures with respect to pure PM.

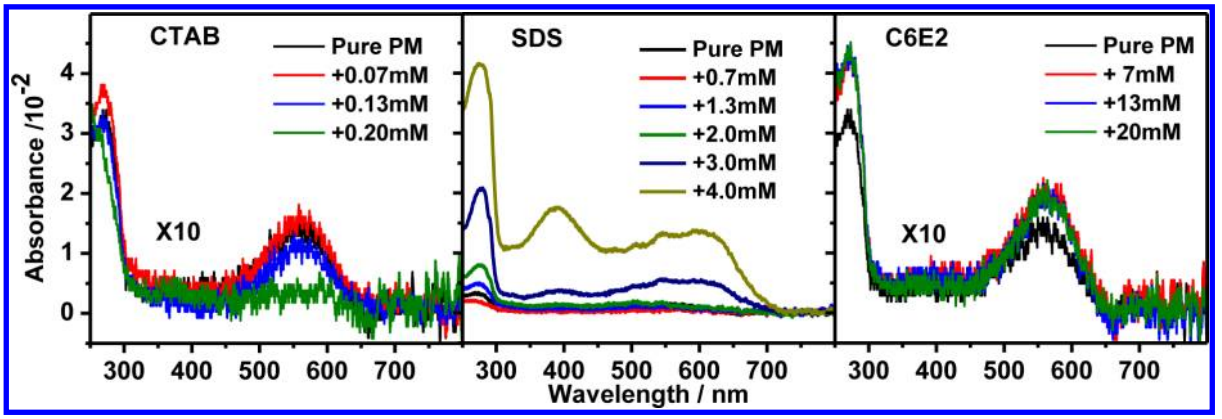

Figure 3. UV−vis absorption spectra of the supernatants of the mixtures in Figure 2 after centrifugation for 15 min at 18 400*g*.

in a single measurement, and three individual measurements were averaged to obtain the zeta potential for each sample.

3. RESULTS

Ultraviolet−visible absorption spectroscopy is used to determine the configuration of bR in the native PM (i.e., to determine if the PM is delipidated[13] or if it is in its monomeric form[11]) by monitoring the absorption maximum attributed to the retinal moiety in the bR interior. CD spectroscopy is utilized to examine the trimeric configuration of the PM integrity according to the biphasic contour.[21] The fluorescence upon excitation of the constituent tryptophans in bR at 280 nm reflects the alteration of the chemical environment around these aromatic residues.[22] Infrared absorption spectroscopy is performed to distinguish the alteration of the secondary structure of bR by analyzing the spectral properties of the amide I and amide II bands.[23,24] Moreover, the zeta potential was also measured because it has been employed to characterize the electrical properties of the protein surface.[25]

3.1. Steady-State UV−vis Absorption Spectra. UV−vis absorption spectroscopy has been extensively utilized in characterizing the electronic transition of the retinal and the aromatic residues of bR in the visible and ultraviolet region, respectively. An intense absorption band at 568 nm is attributed to the light-adapted all-*trans* retinal with an extinction coefficient of 62 700 M^{-1} cm^{-1} at 568 nm.[20,26] A more intense band at 260−280 nm has been ascribed to the superposition of the bands attributed to the aromatic residues of bR, including 8 tryptophans and 11 tyrosines.[27] Upon reduction of the retinal with hydroxylamine under yellow light irradiation, retinal oxime is generated, which has a characteristic absorption maximum at 360 nm.[28] In addition, the hydrolysis of the protonated Schiff base of bR leads to the generation of the free all-*trans* retinal that exhibits an absorption maximum at 390 nm.[29] It should be noted that the surfactants used in this work are spectrally silent from 700 to 280 nm; that is, the observed UV−vis difference of PM upon the addition of surfactants is solely attributed to the structural and conformational alteration of PM and bR.

dx.doi.org/10.1021/jp401254j | *J. Phys. Chem. B* 2013, 117, 6241−6249

The absorption spectra of PM in the presence of CTAB, SDS, and C6E2 of different concentrations are shown in Figure 2a. The corresponding difference spectra of the mixtures with respect to pure PM are shown in Figure 2b. Significant difference was observed upon treatment with the ionic surfactants CTAB and SDS. Upon gradual addition of CTAB, the retinal moiety at 568 nm does not bleach significantly, but there is an increase in the absorbance at the shorter wavelengths. In contrast, the addition of SDS leads to a significant red shift of the retinal band to 600 nm. At higher SDS concentrations, the band at 600 nm disappeared, followed by the generation of a new band at 390 nm, and the absorbance at the shorter wavelengths is decreased as the concentration of SDS is increased. As for the addition of C6E2, no notable difference was observed under our experimental conditions.

In addition to monitoring the mixtures containing PM and surfactants, the solutions were centrifigued to separate the supernatants of the mixtures to investigate the surfactant-induced solubilization of PM and denaturation of bR. The supernatants were collected after 15 min of centrifugation of the mixtures at 18 400*g*, and the corresponding absorption spectra were recorded, as shown in Figure 3. In general, two absorption bands were monitored: the band at 568 nm, which is attributed to the retinal of bR in PM, and the band at 390 nm, which is attributed to free retinal. As the concentration of CTAB was increased, the amount of PM remaining in the supernatant decreased, as indicated by the decrease in the absorbance of the supernatant at 568 nm. However, the addition of SDS leads to the disappearance of the absorption band at 568 nm and the generation of a band at 390 nm, indicating the generation of free retinal. The addition of C6E2 slightly increases the solubility of PM because the absorption at 568 nm increases slightly as the concentration of C6E2 is increased. The detailed mechanisms resulting in the differences in the UV−vis absorption spectra will be discussed in Section 4.

3.2. Circular Dichroism Spectra in the Visible Region. The CD spectra in the visible region are used to verify the trimeric configuration of bR according to the biphasic contour, which exhibits a positive lobe and a negative lobe at shorter and longer wavelengths, respectively, with a crossover at 574 nm.[21,30,31] The magnitude of the molar ellipticity indicates the strength of the coupling of the retinals in the trimeric configuration and is inversely proportional to the cube of the distance of the interactive dipoles.[21] The retinal in monomeric bR exhibits a monophasic contour with a maximum at 550 nm.[21] The observed CD spectra of the surfactant-treated PM solutions, shown in Figure 4, manifested unchanged ellipticity upon treatment with CTAB and C6E2. The preservation of the biphasic lobes and the magnitude of ellipticity indicates that the trimeric configuration was retained in the PM. However, the addition of SDS leads to a monophasic contour with decreased ellipticity. This implies that SDS is able to induce the monomerization of PM and the denaturing of bR.

3.3. Fluorescence Spectra upon Excitation of bR at 280 nm. The fluorescence spectra of tryptophan-containing proteins have been extensively investigated to reveal the coupling of the tryptophans with the surrounding residues and the environment.[32] Upon excitation of the tryptophans in bR at 280 nm, an emission contour was observed from 290 to 400 nm with a maximum at 325 nm. In general, a broad emission contour from 307−355 nm can be characterized as the superposition of several components that are attributed to the exciplex formed between tryptophans and the surrounding

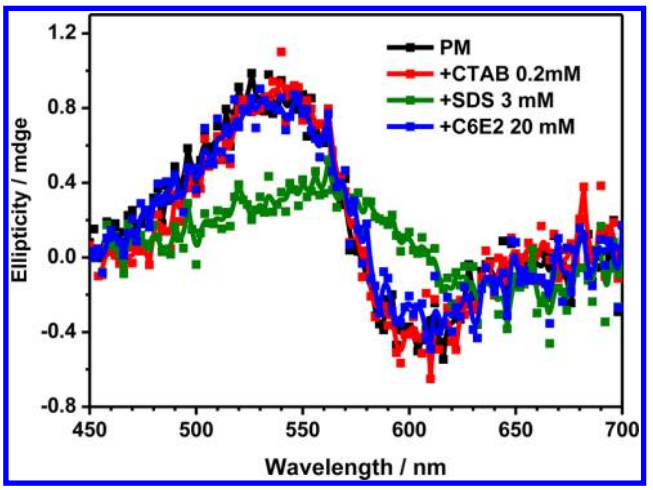

Figure 4. Circular dichroism (CD) spectra of pure PM and the mixtures treated with surfactants.

atoms and water in the electronic excited states, including the isolated excited state (λ_{max} = 308 nm), singly coupled exciplex (λ_{max} = 316 nm), doubly coupled exciplex (λ_{max} = 331 nm), and water-exposed typtophans (λ_{max} = 340−353 nm).[32] In this work, the addition of surfactants altered the emission contour of the fluorescence spectra significantly in terms of the intensity and the spectral shift, as shown in Figure 5. The fluorescence spectra of the surfactant-containing PM mixtures and the supernatants manifested significant difference in comparison

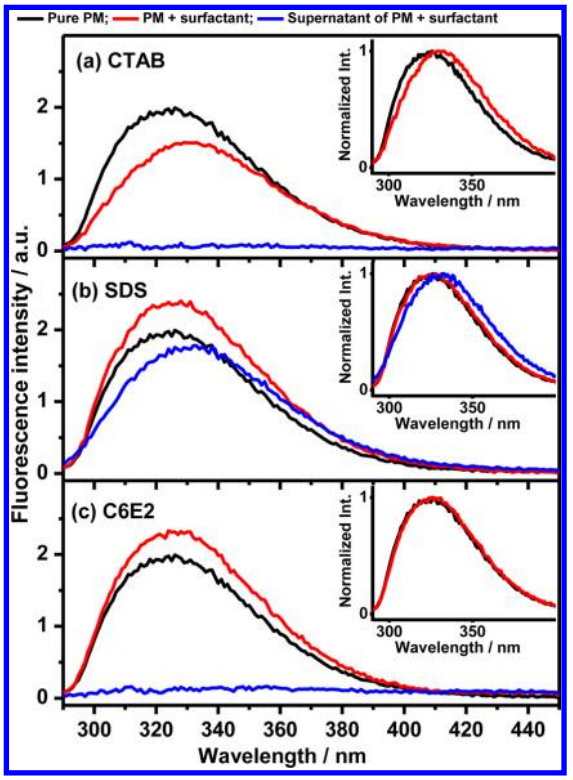

Figure 5. Fluorescence spectra upon excitation at 280 nm of the mixtures containing PM and surfactants (a) 0.2 mM CTAB, (b) 2 mM SDS, and (c) 20 mM C6E2 in aqueous solution, including the pure PM (black trace), freshly made mixture (red trace), and the supernatant of the mixture after centrifugation for 15 min at 18 400*g* (blue trace).

dx.doi.org/10.1021/jp401254j | J. Phys. Chem. B 2013, 117, 6241−6249

with PM. The fluorescence of the mixture of PM and CTAB is less intense than that of pure PM, as shown in Figure 5a. It can also be seen that the supernatant of the PM and CTAB mixture did not manifest a significant fluorescence intensity. In contrast, the fluorescence of the SDS-treated PM, shown in Figure 5b, manifested enhanced emission intensity, and the supernatant also displays fluorescence intensity. It should be noted that the fluorescence contours of the mixture of PM and CTAB and the supernatant of PM and SDS are red-shifted with respect to that of pure PM, as shown in the intensity-normalized traces in the insets. Regarding the treatment with C6E2, the FL intensity is slightly enhanced with an unchanged contour, as shown in Figure 5c. The negligible fluorescence intensity of the supernatants of PM treated with CTAB and C6E2 indicated that the PM rarely dissolves in CTAB and C6E2, whereas SDS is able to solubilize PM in aqueous solution according to the observed increase in the fluorescence intensity of the supernatant.

3.4. Infrared Absorption Spectra. The infrared absorption bands of PM are classified into two groups, those from bR and those from lipids. Several intense bands for bR are attributed to the N−H stretch mode (amide A, 3305 cm^{-1}), bonded N−H stretch (amide B, 3060 cm^{-1}), C═O stretch in the skeleton (amide I, 1660 cm^{-1}), and N−H in-plane bending (amide II, 1545 cm^{-1}).[33,34] The absorption features attributed to lipids can be sorted in terms of the haloarcheal hydrocarbon groups and the head groups, mainly observed at around 3000 and 1200 cm^{-1}, respectively.[24] The infrared spectrum of PM and the corresponding assignment can be found in Figure S1 and Table S1 in the Supporting Information.

In addition to the IR absorption bands of PM, the IR absorption contours of the surfactants are shown in the upper panels of Figure 7. The hydrophobic tails of these surfactants are composed of methylene ($-CH_2-$) and methyl ($-CH_3$) groups, and the corresponding stretching modes are mainly at ca. 3000 cm^{-1}. A characteristic band at 960 cm^{-1} is attributed to the CH_3-N^+ stretching mode of CTAB.[35] Two intense bands at 1250 and 1219 cm^{-1} and a less intense band at 1080 cm^{-1} are attributed to the degenerate asymmetric stretching and symmetric stretching of the sulfate ($-OSO_3^-$) of SDS, respectively.[36] Although the analysis of the vibrational modes of C6E2 has not been reported, the assignments can be carried out based on its analogue ethylene glycol monoethyl ether, $C_2H_5(C_2H_4O)OH$.[37] A broad band at 3445 cm^{-1} is attributed to the H-bonded OH stretching mode of C6E2. Bands at 1450−1500 cm^{-1} are attributed to the bending modes of methyl and methylene groups. A band at 1370 cm^{-1} is attributed to the wagging mode of the $-C_2H_4O-$ group. The detailed assignments are listed in Table S2 in the Supporting Information.

The difference between the IR spectra of the surfactant-treated PM and the pure PM indicates the probability of the surfactant attachment to the PM surface and the subsequent surfactant-induced alteration of the secondary structure of bR. Previous report revealed that the flexibility of the protein is indicated by the bandwidth of the amide I band and by the absorbance ratio of the amide I band/amide II band. A narrow bandwidth of the amide I band with slightly reduced absorbance for amide II indicates a compressed configuration, whereas a broadened band represents a loose structure,[38] composed of diverse secondary structures in β-sheet or random-coil components. Although hydration leads to an alteration of the infrared absorption pattern,[39] the comparison in this study has been carried out based on the same dehydrated condition. Moreover, a previous report indicated that the randomly oriented and highly oriented PM films show similar depolarization ratios in the amide I, amide II, and amide A bands.[40] Therefore, the observed spectral difference truly resulted from the surfactant-induced structural changes of bR and PM instead of orientation effect. The infrared absorption spectra of the surfactant-treated PM are distinct and will be discussed in the latter section.

3.5. Zeta Potentials. The measurements of the zeta potential of the surfactant-treated PM at pH 7.4 reflected the alteration of the surface charge distribution, as shown in Table 1. The zeta potential of the pure PM is negative due to the negatively charged lipids at the peripherals of the trimmeric PM. When CTAB was added in the PM suspensions, the value of the zeta potential remained negative but decreased in the magnitude. This implies that the negative charge on the PM surface was partially neutralized by the cationic quaternary ammonium head of CTAB. However, the zeta potential of the SDS-treated PM was much more negative than that of pure PM. The attachment of the SDS on the PM surface leads to the accumulation of the negative charge from the anionic sulfate head of the SDS. Regarding C6E2, its neutrality leads to an unchanged surface charge of PM. Redistribution of the charge of the PM surface leads to the distinct effects, such as solubilization and aggregation, and the details will be addressed in the latter section.

Table 1. Zeta Potentials of the Pure Purple Membrane and the Surfactant-Treated Purple Membranes

sample	zeta potential/mV
water	−2.8 ± 2.1
PM	−52.0 ± 1.2
PM + 0.2 mM CTAB	−41.4 ± 0.9
PM + 2 mM SDS	−64.4 ± 3.0
PM + 20 mM C6E2	−50.2 ± 1.1

4. DISCUSSION

4.1. Effects of the Cationic Surfactant CTAB. In comparison with the pure PM, the addition of CTAB to the PM suspension leads to a distinct difference in the UV−vis absorption spectrum, as shown in Figure 2a. As the concentration of CTAB is gradually increased, the absorption of the retinal moiety at 568 nm is not greatly changed, whereas there is an increase in the absorption baseline at shorter wavelengths, as shown in the difference spectra in Figure 2b. After centrifugation (15 min at 18 400*g*), the spectra of the supernatant of the PM and CTAB mixture show a slightly reduced absorbance in comparison with that of pure PM as the concentration of CTAB is increased (Figure 3). The reduction in absorbance intensity following centrifugation indicates that some of the PM was removed from the solution into the pellet. It can therefore be deduced that the addition of CTAB to the PM suspension reduces the solubility of PM and leads to the aggregation of PM. The increase in size of the PM aggregate enhances the Rayleigh scattering and causes the increase in absorbance at shorter wavelengths. Similarly, an analogue cationic surfactant dodecyl trimethyl ammonium chloride (DTAC) below its CMC was also employed in high-resolution electron cryo-microscopy to fuse small PM aggregates to form larger 2D crystals.[41] However, the bR in the aggregated PM still

dx.doi.org/10.1021/jp401254j | J. Phys. Chem. B 2013, 117, 6241−6249

preserved its trimeric configuration because the CD spectrum exhibits a biphasic characteristic without depletion (Figure 4). Additionally, the fluorescence of the mixture of bR and CTAB is less intense and shows a bathochromic shift in comparison with that of pure bR (Figure 5a). The reduced fluorescence intensity presumably results from the PM aggregate scattering, the incident excitation, and the fluorescence emission. The aggregated PM is less flexible, and the enhanced couplings between the tryptophans and the nearby residues lead to a reduction in the fluorescence intensity as well. Meanwhile, aggregation of the PM reduced the amount of isolated tryptophans in bR; therefore, the fluorescence emission contour exhibits a bathochromic shift, as shown in the inset of Figure 5a.

As previously mentioned, the amount of PM left in the supernatant decreased upon the addition of CTAB. The differences in the infrared absorption spectra of the pellets of the pure PM (black) and PM+CTAB mixture (red), as shown in lower panel of Figure 7a with the difference spectra in the insets, offer evidence of the CTAB attachment to the PM surface and the corresponding structural alteration of bR. Two extra bands at 2853 cm^{-1} and 2924 cm^{-1} (as denoted by the dots) were observed in the CTAB-treated PM that are coincident with the bands attributed to methylene ($-CH_2-$) stretch modes of CTAB. Moreover, the relative absorbance of amide I and amide II and their bandwidths, as shown in the overlay in the right inset of Figure 7a, were also altered but without spectral shift. The narrowed bandwidth of amide I and a decrease in the intensity of the amide II band indicates a compressed structure of bR.[38] The IR absorption spectra are accordingly consistent with the UV−vis absorption and fluorescence spectra that manifested aggregated PM and compressed bR upon the treatment of PM suspension with CTAB.

CTAB is composed of a 16-carbon hydrophobic tail and a quaternary ammonium hydrophilic head, as shown in Figure 1. Miller et al. have demonstrated that a surfactant is able to adhere to a protein surface via the hydrophobic and hydrophilic interaction with the constituent residues of the protein.[42] The negative charges of the phosphate and sulfate hydrophilic heads of the native PGP and GLS lipids in PM are able to interact with the positively charged quaternary ammonium of CTAB via electrostatic interactions when [CTAB] is lower than its CMC, as illustrated in Figure 8. The reduced magnitude of the negative zeta potential of the CTAB-treated PM also supports this conclusion. The neutralization of the surface charge of PM by CTAB leads to the decrease in the solubility of PM and its further aggregation.

4.2. Effects of the Anionic Surfactant SDS. SDS is composed of a 12-carbon hydrophobic tail and a sulfate hydrophilic head, as shown in Figure 1. The addition of SDS to PM suspensions is expected to lead to the opposite phenomenon compared with CTAB. Upon gradual addition of SDS to the PM suspensions, the UV−vis absorbance spectra showed a depletion of the band at 568 nm, an increased absorbance at 600 nm, and unchanged absorbance at 280 nm (Figure 2a). The observed new contour at 600 nm implies that the addition of SDS causes a loose secondary structure of bR. This result is consistent with the previous report by Padrós et al. that a decrease in the interaction between the protonated Schiff base and the surrounding counterion leads to the generation of a contour with a maximum at ca. 600 nm.[17] As more SDS was added (up to a [SDS] of 4 mM), a band at 390 nm was observed, indicating free retinal.[29] This observation is consistent with London and Khorana's report that the 390 nm species has lost most interaction with the apoprotein.[43] In addition, the UV−vis absorption spectra of the supernatant of the SDS and PM mixture after centrifugation (15-min at 18,400 g) showed an increase in the absorbance at 390 nm with an increasing concentration of SDS. This indicates that the gradual addition of SDS truly resulted in the increased solubilization of PM and the generation of free retinal (Figure 3). The observed UV−vis absorption spectra of the mixture of SDS and PM and its supernatant manifested that SDS is able to solubilize the PM suspension and leads to the denaturing of bR and the generation of the free retinal as the concentration of SDS increased.

In addition to the UV−vis absorption spectra, the concentration-dependent fluorescence spectra of the mixtures of PM and SDS and the supernatants were collected, as shown in Figure 6a,b, respectively. The intensities of the fluorescence

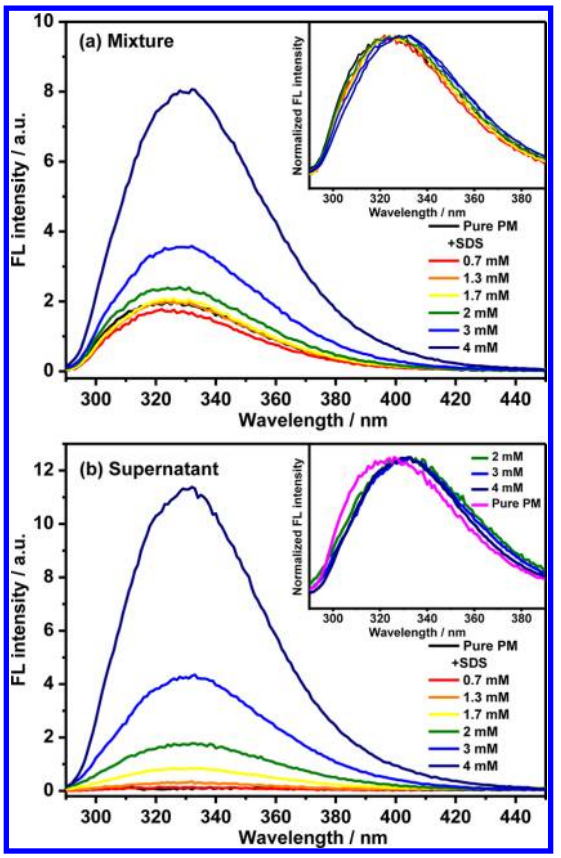

Figure 6. Steady-state fluorescence spectra upon excitation at 280 nm of (a) the mixtures of PM and SDS and (b) the supernatant of the mixture at varied SDS concentrations. The normalized traces are plotted in the insets.

of the mixtures and supernatants both increased as the concentration of SDS increased. The increase in the fluorescence implies a decrease in the coupling between the tryptophans and the surrounding residues in bR and retinal. This is attributed to the SDS-assisted solubilization of PM that manifested a loose structure of bR. In addition, a red shift of the fluorescence emission contour was observed and attributed to the exposure of the tryptophans to water.[32] As the concentration of SDS is gradually increased, an abrupt fluorescence emission intensity increase in the bR/SDS

dx.doi.org/10.1021/jp401254j | J. Phys. Chem. B 2013, 117, 6241−6249

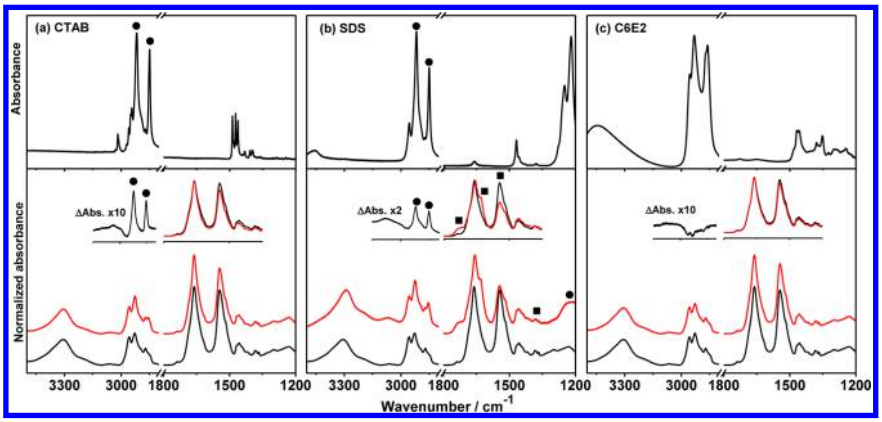

Figure 7. Infrared spectra of the PM treated with surfactants (a) 0.2 mM CTAB, (b) 2 mM SDS, and (c) 20 mM C6E2. The absorption contours of the pure surfactants are shown in the upper panels. The spectra of the pure PM and surfactant-treated PM are shown in the lower panels, with the difference spectra and the zoomed-in spectra of the amide I and amide II bands in the insets. The dots and squares denote the extra bands attributed to the surfactants and new bR characteristics, respectively.

mixture, and the supernatant was observed at [SDS] = 3 mM. This fluorescence emission intensity increase is attributed to the SDS-induced alteration of the structure of the bR. The diminished coupling of the ensemble of tryptophans with the surrounding molecules and the retinal in bR's interior leads to an insufficient energy transfer via nonradiative processes, and the emission intensity is therefore greatly increased.

The infrared absorption spectrum of the dried film of the supernatant of the bR/SDS mixture, as shown by the red trace in the lower panel of Figure 7b with the difference spectra in the insets, exhibits significant differences in comparison with pure PM (black trace). Three extra bands (denoted in dots) were ascribed to the stretches of the methylene and $-SO_4^-$ of SDS at 2925, 2855, and 1219 cm^{-1}, respectively.[36] The broadening of the amide I and amide II bands exhibits the decreased homogeneity of the bR secondary structure, that is, in association with the generation of the β-sheet and random-coil components. An extra band at 1630 cm^{-1} was generated with a decreased absorbance for the amide II band. This is presumably attributed to an intramolecular antiparallel β-sheet[23] that is generated during the SDS-induced conformational change of bR when peptide-plane flipping occurs in the unfolding and refolding of polypeptides.[44] This is also consistent with the report by Kluge et al., where these changes indicated that an unfolded bR underwent the refolding process.[45] Moreover, a spectral shift of the amide I band from 1660 to 1657 cm^{-1} coupled to a decreased intensity of the amide II band indicates the conversion of the α_{II}-helical structure to α_I-helices, which manifests a loose bR structure.[24] In addition, the absorbance of band at 1740 cm^{-1}, attributed to the C═O stretch mode of −COOH, is increased, and the absorbance at 1390 cm^{-1}, which is attributed to the C═O stretch of $-COO^-$,[24] is concomitantly decreased. This suggests that the buried deprotonated residues of bR, such as glutamate and aspartate, are exposed to water and are partially protonated in the loose bR structure. We have summarized our observations on the interaction of PM and SDS in Figure 8. The SDS adhered to the PM surface via hydrophobic interactions and resulted in an increased magnitude of the negative zeta potential. The accumulation of the negative charges of SDS on the PM surface increases the solubility of PM and leads to a loose PM structure. As the concentration of SDS is increased to more than 3 mM, the PM becomes monomerized and the secondary structure of bR is destroyed,

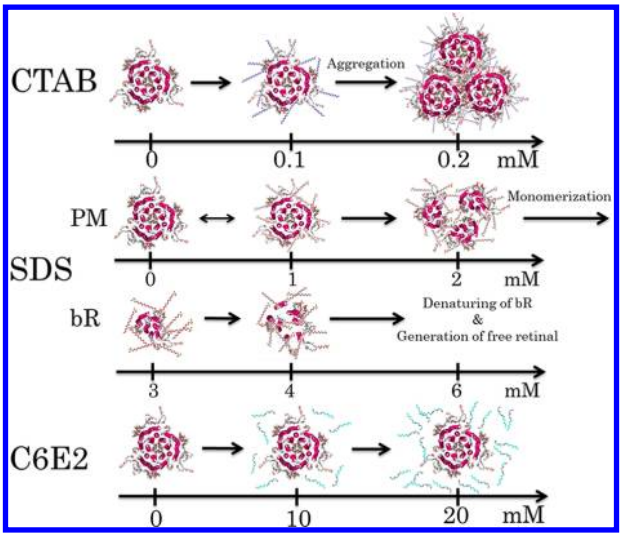

Figure 8. Schematic explanation of the interaction of PM with the various surfactants at different concentrations. The protein structure is redrawn according to PDB ID 1c3w (ref 47).

coupled to the hydrolysis of the protonated Schiff base and the generation of free retinal.

4.3. Effects of the Neutral Surfactant C6E2. In comparison with the effects of the ionic surfactants CTAB and SDS, C6E2 plays only a minor role in perturbing the structure of PM and bR. The addition of C6E2 leads to minute solubilization, indicated by the small but insignificant increase in absorbance attributed to PM in the supernatant (Figure 3). Meanwhile, the fluorescence intensity was slightly enhanced but showed no spectral shift (Figure 5c). These results imply that C6E2 is mild and is not able to sufficiently solubilize PM. The unchanged CD contour, as shown in Figure 4, also supports the aforementioned claim. The infrared absorption spectrum of the pellets of the mixture of PM and C6E2 is practically identical to that of the pure PM (Figure 7). There were no extra bands in the difference spectrum, which indicates that C6E2 rarely attached to the PM. Moreover, the nearly unchanged absorption contours of the amide I and amide II bands indicated that C6E2 is rarely able to alter the PM structure.

C6E2 is neutral and composed of a six-carbon alkyl tail, two units of ethylene glycol, and one terminal hydroxyl group, as

dx.doi.org/10.1021/jp401254j | J. Phys. Chem. B 2013, 117, 6241−6249

shown in Figure 1. The short hydrophobic alkyl tail and noncharged hydrophilic head suppressed the capability of C6E2 to attach to the PM surface, even when the concentration of C6E2 was as high as 20 mM. In comparison, the neutral surfactant Triton X-100, which is composed of more ethylene glycol units, is able to remove the lipids from the PM and leads to the monomerization of PM.[46] As a result, we conclude that neutral surfactants with shorter hydrophobic tails and fewer hydrophilic heads are less effective in perturbing the structural integrity of PM and rarely attach to the PM surface, as illustrated in Figure 8.

5. CONCLUSIONS

The interaction of PM and bR with various surfactants has been investigated using steady-state spectroscopy. The quaternary ammonium hydrophilic head of the cationic surfactant CTAB is able to neutralize the negatively charged lipids on the PM surface. The subsequently reduced hydrophilicity leads to the aggregation of the PM. On the contrary, the addition of SDS results in an increased solubility of PM and a resultant loose crystalline structure of PM as SDS attaches to its surface. As the concentration of SDS is increased, a further alteration of the secondary structure of bR and the hydrolysis of the protonated Schiff base occurred. The addition of the neutral surfactant C6E2 played only a minor role in perturbing the structures and configuration of the PM and bR. We conclude that the addition of surfactants leads to either the solubilization or aggregation of PM, depending on the signs of the charged hydrophilic heads of the surfactants and the charges of the protein surface.

■ ASSOCIATED CONTENT

Ⓢ Supporting Information

Infrared spectrum of the dried film of the PM and the assignments of the vibrational modes of bR and lipids moiety in the PM and the surfactants CTAB, SDS, and C6E2. This material is available free of charge via the Internet at http://pubs.acs.org.

■ AUTHOR INFORMATION

Corresponding Author

*Phone: +886-3-5715131, ext. 33396. Fax: +886-3-5711082. E-mail: lkchu@mx.nthu.edu.tw.

Notes

The authors declare no competing financial interest.

■ ACKNOWLEDGMENTS

National Science Council of Taiwan (NSC101-2113-M-007-016-MY2) and Ministry of Education of R.O.C. (Grant No. 101N2011E1) provided support for this research.

■ REFERENCES

(1) Oesterhelt, D.; Stoeckenius, W. Rhodopsin-like Protein from the Purple Membrane of *Halobacterium halobium*. *Nat. New Biol.* **1971**, *233*, 149−52.

(2) Lanyi, J. K. Bacteriorhodopsin as a Model for Proton Pumps. *Nature* **1995**, *375*, 461−463.

(3) Cartailler, J.-P.; Luecke, H. X-ray Crystallographic Analysis of Lipid-Protein Interactions in the Bacteriorhodopsin Purple Membrane. *Annu. Rev. Biophys. Biomol. Struct.* **2003**, *32*, 285−310.

(4) Corcelli, A.; Lattanzio, V. M. T.; Mascolo, G.; Papadia, P.; Fanizzi, F. Lipid-Protein Stoichiometries in a Crystalline Biological Membrane: NMR Quantitative Analysis of the Lipid Extract of the Purple Membrane. *J. Lipid Res.* **2002**, *43*, 132−140.

(5) Baudry, J.; Tajkhorshid, E.; Molnar, F.; Phillips, J.; Schulten, K. Molecular Dynamics Study of Bacteriorhodopsin and the Purple Membrane. *J. Phys. Chem. B* **2001**, *105*, 905−918 and references therein.

(6) Dracheva, S.; Bose, S.; Hendler, R. W. Chemical and Functional Studies on the Importance of Purple Membrane Lipids in Bacteriorhodopsin Photocycle Behavior. *FEBS Lett.* **1996**, *382*, 209−212.

(7) Teissié, J.; Prats, M.; LeMassu, A.; Stewart, L. C.; Kates, M. Lateral Proton Conduction in Monolayers of Phospholipids from Extreme Halophiles. *Biochemistry* **1990**, *29*, 59−65.

(8) Joshi, M. K.; Dracheva, S.; Mukhopadhyay, A. K.; Bose, S.; Hendler, R. W. Importance of Specific Native Lipids in Controlling the Photocycle of Bacteriorhodopsin. *Biochemistry* **1998**, *37*, 14463−14470.

(9) del Río, E.; González-Mañas, J. M.; Gurtubay, J.-I. G; Goñi, F. M. On the Mechanism of Bacteriorhodopsin Solubilization by Surfactants. *Arch. Biochem. Biophys.* **1991**, *291*, 300−306.

(10) Dencher, N. A.; Heyn, M. P. Formation and Properties of Bacteriorhodopsin Monomers in the Non-Ionic Detergents Octyl-β-D-Glucoside and Triton X-100. *FEBS Lett.* **1978**, *96*, 322−326.

(11) Wang, J.; Link, S.; Heyes, C. D.; El-Sayed, M. A. Comparison of the Dynamics of the Primary Events of Bacteriorhodopsin in Its Trimeric and Monomeric States. *Biophys. J.* **2002**, *83*, 1557−1566.

(12) Heyes, C. D.; El-Sayed, M. A. Proton Transfer Reactions in Native and Deionized Bacteriorhodopsin upon Delipidation and Monomerization. *Biophys. J.* **2003**, *85*, 426−434.

(13) Szundi, I.; Stoeckenius, W. Effect of Lipid Surface Charges on the Purple-to-Blue Transition of Bacteriorhodopsin. *Proc. Natl. Acad. Sci. U. S. A.* **1987**, *84*, 3681−3684.

(14) Chu, L.-K.; El-Sayed, M. A. Kinetics of the M-Intermediate in the Photocycle of Bacteriorhodopsin upon Chemical Modification with Surfactants. *Photochem. Photobiol.* **2010**, *86*, 316−323.

(15) Chu, L.-K.; El-Sayed, M. A. Bacteriorhodopsin O-State Photocycle Kinetics: A Surfactant Study. *Photochem. Photobiol.* **2010**, *86*, 70−76.

(16) Tan, E. H. L.; Birge, R. R. Correlation between Surfactant/Micelle Structure and the Stability of Bacteriorhodopsin in Solution. *Biophys. J.* **1996**, *70*, 2385−2395.

(17) Padrós, E.; Duñach, M.; Sabés, M. Induction of the Blue Form of Bacteriorhodopsin by Low Concentrations of Sodium Dodecyl Sulfate. *Biochim. Biophys. Acta* **1984**, *769*, 1−7.

(18) Krishnamani, V.; Hegde, B. G.; Langen, R.; Lanyi, J. K. Secondary and Tertiary Structure of Bacteriorhodopsin in the SDS Denatured State. *Biochemistry* **2012**, *51*, 1051−1060.

(19) Oesterhelt, D.; Stoeckenius, W. Isolation of the Cell Membrane of *Halobacterium halobium* and Its Fractionation into Red and Purple Membrane. *Methods Enzymol.* **1974**, *31*, 667−678.

(20) Rehorek, M.; Heyn, M. P. Binding of all-*trans*-Retinal to the Purple Membrane. Evidence for Cooperativity and Determination of the Extinction Coefficient. *Biochemistry* **1979**, *18*, 4977−4983.

(21) Cassim, J. Y. Unique Biphasic Band Shape of the Visible Circular Dichroism of Bacteriorhodopsin in Purple Membrane: Excitons, Multiple Transitions or Protein Heterogeneity? *Biophys. J.* **1992**, *63*, 1432−1442.

(22) Reshetnyak, Y. K.; Burstein, E. A. Decomposition of Protein Tryptophan Fluorescence Spectra into Log-Normal Components. II. The Statistical Proof of Discreteness of Tryptophan Classes in Proteins. *Biophys. J.* **2001**, *81*, 1710−1734.

(23) Lee, D. C.; Chapman, D. Infrared Spectroscopic Studies of Biomembranes and Model Membranes. *Biosci. Rep.* **1986**, *6*, 235−256.

(24) Barnett, S. M.; Dracheva, S.; Hendler, R. W.; Levin, I. W. Lipid-Induced Conformational Changes of an Integral Membrane Protein: An Infrared Spectroscopic Study of the Effects of Triton X-100 Treatment on the Purple Membrane of *Halobacterium halobium* ET1001. *Biochemistry* **1996**, *35*, 4558−4567.

(25) Bowen, W. R.; Hall, N. J.; Pan, L.-C.; Sharif, A. O.; Williams, P. M. The Relevance of Particle Size and Zeta-Potential in Protein Processing. *Nat. Biotechnol.* **1998**, *16*, 785−787.

(26) Becher, B.; Tokunaga, F.; Ebrey, T. G. Ultraviolet and Visible Absorption Spectra of the Purple Membrane Protein and the Photocycle Intermediates. *Biochemistry* **1978**, *17*, 2293−2300.
(27) Marti, T. Refolding of Bacteriorhodopsin from Expressed Polypeptide Fragments. *J. Biol. Chem.* **1998**, *273*, 9312−9322.
(28) Subramaniam, S.; Marti, T.; Rösselet, S. J.; Rothschild, K. J.; Khorana, H. G. The Reaction of Hydroxylamine with Bacteriorhodopsin Studied with Mutants that Have Altered Photocycles: Selective Reactivity of Different Photointermediates. *Proc. Natl. Acad. Sci. U. S. A.* **1991**, *88*, 2583−2587.
(29) Schlebach, J. P.; Cao, Z.; Bowie, J. U.; Park, C. Revisiting the Folding Kinetics of Bacteriorhodopsin. *Protein Sci.* **2012**, *21*, 97−106.
(30) Heyn, M. P.; Bauer, P.-J.; Dencher, N. A. A Natural CD Label to Probe the Structure of the Purple Membrane from *Halobacterium halobium* by Means of Exciton Coupling Effects. *Biochem. Biophys. Res. Commun.* **1975**, *67*, 897−903.
(31) Becher, B.; Cassim, J. Y. Effects of Light Adaptation on the Purple Membrane Structure of *Halobacterium halobium*. *Biophys. J.* **1976**, *16*, 1183−1200.
(32) Reshetnyak, Y. K.; Koshevnik, Y.; Burstein, E. A. Decomposition of Protein Tryptophan Fluorescence Spectra into Log-Normal Components. III. Correlation between Fluorescence and Microenvironment Parameters of Individual Tryptophan Residues. *Biophys. J.* **2001**, *81*, 1735−1758.
(33) Rothschild, K. J.; Clark, N. A. Polarized Infrared Spectroscopy of Oriented Purple Membrane. *Biophys. J.* **1979**, *25*, 473−487.
(34) Asai, M.; Tsuboi, M.; Shimanouchi, T.; Mizushima, S.-I. Infrared Spectra of Polypeptides and Related Compounds. I. *J. Phys. Chem.* **1955**, *59*, 322−325.
(35) Chen, L.; Lu, G. Direct Electrochemistry and Electrocatalysis of Hybrid Film Assembled by Polyelectrolyte−Surfactant Polymer, Carbon Nanotubes and Hemoglobin. *J. Electroanal. Chem.* **2006**, *597*, 51−59.
(36) Kartha, V. B.; Leitch, L. C.; Mantsch, H. H. Infrared and Raman Spectra of Alkali Palmityl Sulfates. *Can. J. Chem.* **1984**, *62*, 128−132.
(37) Nguyen, T. T.; Raupach, M.; Janik, L. J. Fourier-Transform Infrared Study of Ethylene Glycol Monoethyl Ether Adsorbed on Montmorillonite: Implications for Surface Area Measurements of Clays. *Clays Clay Miner.* **1987**, *35*, 60−67.
(38) Hendler, R. W.; Barnett, S. M.; Dracheva, S.; Bose, S.; Levin, I. W. Purple Membrane Lipid Control of Bacteriorhodopsin Conformational Flexibility and Photocycle Activity. *Eur. J. Biochem.* **2003**, *270*, 1920−1925.
(39) Váró, G.; Eisenstein, L. Infrared Studies of Water Induced Conformational Changes in Bacteriorhodopsin. *Eur. Biophys. J.* **1987**, *14*, 163−168.
(40) Wang, J. Vectorially Oriented Purple Membrane: Characterization by Photocurrent Measurement and Polarized-Fourier Transform Infrared Spectroscopy. *Thin Solid Films* **2000**, *379*, 224−229.
(41) Henderson, R.; Baldwin, J. M.; Ceska, T. A.; Zemlin, F.; Beckmann, E.; Downing, K. H. Model for the Structure of Bacteriorhodopsin Based on High-Resolution Electron Cryo-Microscopy. *J. Mol. Biol.* **1990**, *213*, 899−929.
(42) Miller, R.; Fainerman, V. B.; Makievski, A. V.; Krägel, J.; Grigoriev, D. O.; Kazakov, V. N.; Sinyachenko, O. V. Dynamics of Protein and Mixed Protein/Surfactant Adsorption Layers at the Water/Fluid Interface. *Adv. Colloid Interface Sci.* **2000**, *86*, 39−82.
(43) London, E.; Khorana, H. G. Denaturation and Renaturation of Bacteriorhodopsin in Detergents and Lipid-Detergent Mixtures. *J. Biol. Chem.* **1982**, *257*, 7003−7011.
(44) Hayward, S. Peptide-Plane Flipping in Proteins. *Protein Sci.* **2001**, *10*, 2219−2227.
(45) Kluge, T.; Olejnik, J.; Smilowitz, L.; Rothschild, K. J. Conformational Changes in the Core Structure of Bacteriorhodopsin. *Biochemistry* **1998**, *37*, 10279−10285.
(46) Reynolds, J. A.; Stoeckenius, W. Molecular Weight of Bacteriorhodopsin Solubilized in Triton X-100. *Proc. Natl. Acad. Sci. U. S. A.* **1977**, *74*, 2803−2804.
(47) Luecke, H.; Schobert, B.; Richter, H.-T.; Cartailler, J.-P.; Lanyi, J. K. Structure of Bacteriorhodopsin at 1.55 Å Resolution. *J. Mol. Biol.* **1999**, *291*, 899−911.